Complex-temperature singularities in the $d = 2$ Ising model: triangular and honeycomb lattices

Victor Matveev† and Robert Shrock‡

Institute for Theoretical Physics, State University of New York, Stony Brook, NY 11794-3840, USA

Abstract. We study complex-temperature singularities of the Ising model on the triangular and honeycomb lattices. We first discuss the complex-T phases and their boundaries. From exact results, we determine the complex-T singularities in the specific heat and magnetization. For the triangular lattice we discuss the implications of the divergence of the magnetization at the point $u = -\frac{1}{3}$ (where $u = z^2 = e^{-4K}$) and extend a previous study by Guttmann of the susceptibility at this point with the use of differential approximants. For the honeycomb lattice, from an analysis of low-temperature series expansions, we have found evidence that the uniform and staggered susceptibilities $\bar{\chi}$ and $\bar{\chi}^{(a)}$ both have divergent singularities at $z = -1 \equiv z_\ell$, and our numerical values for the exponents are consistent with the hypothesis that the exact values are $\gamma'_\ell = \gamma'_{\ell,a} = \frac{5}{2}$. The critical amplitudes at this singularity were calculated. Using our exact results for α' and β together with numerical values for γ' from series analyses, we find that the exponent relation $\alpha' + 2\beta + \gamma' = 2$ is violated at $z = -1$ on the honeycomb lattice; the right-hand side is consistent with being equal to 4 rather than 2. The connections of the critical exponents at these two singularities on the triangular and honeycomb lattice are discussed.

1. Introduction

In this paper we study complex-temperature (CT) singularities of the (isotropic, nearest-neighbour, spin-$\frac{1}{2}$) Ising model on the triangular and honeycomb lattices. There are several reasons for studying the properties of statistical mechanical models with the temperature variable generalized to take on complex values. First, one can understand more deeply the behaviour of various thermodynamic quantities by seeing how they behave as analytic functions of complex temperature; indeed, CT singularities can significantly influence the behaviour for physical values of the temperature. Second, one can see how the physical phases of a given model generalize to regions in appropriate complex-temperature variables. Third, a knowledge of the complex-temperature singularities of quantities which have not been calculated exactly, such as the susceptibility of the 2D Ising model, helps in the search for exact, closed-form expressions for these quantities. The natural boundaries of the free energy for the 2D (square lattice) Ising model were first given in [1] (see also [2]). Early studies of CT singularities in the 2D and 3D Ising model were motivated by their connection with partition function zeros [1–3] and by their effect on series analyses at the physical critical point [4–6]. Other previous works on CT properties of the 2D Ising model include [7–9]§.

---

† E-mail address: vmatveev@max.physics.sunysb.edu
‡ E-mail address: shrock@max.physics.sunysb.edu
§ We also note that (i) complex-temperature properties of anisotropic 2D Ising models have been discussed in [10]; (ii) partition function zeros of some Potts models (the Ising model being the two-state case) have been discussed, e.g. in [11, 12]; and (iii) a different approach to the effort to calculate the exact 2D Ising susceptibility is via inversion relations [13].

2. Complex-temperature extensions of physical phases

Here we discuss the complex-temperature phase diagrams. Our notation follows that in our previous paper [9], to which we refer the reader; we only recall that $z = e^{-2K}$, $u = z^2$ and $v = \tanh K$, where $K = \beta J$ and $\beta = (k_B T)^{-1}$. It will be convenient to use the reduced susceptibility $\bar{\chi} = \beta^{-1}\chi$. Following the calculations of the (zero-field) free energy f [14] of the square-lattice Ising model, f was calculated for the triangular (t) and honeycomb (hc) lattices [15]. The spontaneous magnetization M, first derived for the square lattice [16], was calculated for the t and hc lattices in [17, 18], respectively. These works made use of the geometric duality between the triangular and honeycomb lattices and the associated star–triangle relation connecting the Ising model on these lattices (e.g. [19]). Two elliptic modulus variables appropriate for the triangular (t) and honeycomb (hc) lattices are

$$k_{<,t} = \frac{4u^{3/2}}{(1 + 3u)^{1/2}(1 - u)^{3/2}} \tag{2.1}$$

and

$$k_{<,hc} = \frac{4z^{3/2}(1 - z + z^2)^{1/2}}{(1 - z)^3(1 + z)} \tag{2.2}$$

together with $k_{>,\Lambda} = k_{<,\Lambda}^{-1}$ for $\Lambda = t$, hc.

As before (see equations (2.10) and (2.11) of [9]), it is convenient to discuss the CT phase diagram in the variables z or v since these remove an infinite repetition of phases in the complex K plane under certain imaginary shifts of K. The requisite CT extensions of the physical phases can be seen by using the exact expressions for the (reduced) free energy f ($f = -\beta F = \lim_{N_s \to \infty} N_s^{-1} \ln Z$) for the triangular lattice [15],

$$f_t = \ln 2 + \frac{1}{2} \int_{-\pi}^{\pi} \int_{-\pi}^{\pi} \frac{d\theta_1\,d\theta_2}{(2\pi)^2} \ln[C^3 + S^3 - SP(\theta_1, \theta_2)] \tag{2.3}$$

and honeycomb lattice,

$$f_{hc} = \ln 2 + \frac{1}{4} \int_{-\pi}^{\pi} \int_{-\pi}^{\pi} \frac{d\theta_1\,d\theta_2}{(2\pi)^2} \ln\{\tfrac{1}{2}[C^3 + 1 - S^2 P(\theta_1, \theta_2)]\} \tag{2.4}$$

where $C = \cosh(2K)$, $S = \sinh(2K)$, and

$$P(\theta_1, \theta_2) = \cos\theta_1 + \cos\theta_2 + \cos(\theta_1 + \theta_2). \tag{2.5}$$

The function $P(\theta_1, \theta_2)$ ranges from a maximum value of 3 at $\theta_1 = \theta_2 = 0$ to a minimum value of $-\frac{3}{2}$ at $\theta_1 = \theta_2 = 2\pi/3$. The continuous locus of points where the free energy is non-analytic is comprised of points where the argument of the logarithm in f vanishes†. Some of these points form boundaries of complex-temperature phases, while others form arcs or line segments which terminate in the interiors of phases and hence do not separate any phases. Expressed in terms of low-temperature variables,

$$f_t = 3K + \frac{1}{2} \int_{-\pi}^{\pi} \int_{-\pi}^{\pi} \frac{d\theta_1\,d\theta_2}{(2\pi)^2} \ln[(1 + 3u^2) - 2u(1 - u)P(\theta_1, \theta_2)] \tag{2.6}$$

and

$$f_{hc} = \frac{3}{2}K + \frac{1}{4} \int_{-\pi}^{\pi} \int_{-\pi}^{\pi} \frac{d\theta_1\,d\theta_2}{(2\pi)^2}$$
$$\times \ln[(1 + z)^2\{(1 - 2z + 6z^2 - 2z^3 + z^4) - 2z(1 - z)^2 P(\theta_1, \theta_2)\}]. \tag{2.7}$$

---

† The free energy is trivially infinite at $K = \pm\infty$; since these are isolated points and hence do not form part of a boundary separating phases, they will not be important here.

(The fact that the log in the integral in (2.7) involves a polynomial in z rather than u is due to the odd coordination number $q = 3$ of the hc lattice.) The respective arguments of the logarithms in (2.6) and (2.7) vanish along the curves defined by the solutions to the equations

$$1 + 3u^2 - 2u(1 - u)x = 0 \tag{2.8}$$

and

$$(1 - 2z + 6z^2 - 2z^3 + z^4) - 2z(1 - z)^2 x = 0 \tag{2.9}$$

for $-\frac{3}{2} \leqslant x \leqslant 3$, where $x = P(\theta_1, \theta_2)$. (Note that the curve defined by the solution to equation (2.9) contains the isolated point $z = -1$ at which the initial factor, $(1 + z)^2$, in the log in equation (2.7) vanishes.) The solution of (2.8) consists of the union of the circle

$$u = -\tfrac{1}{3} + \tfrac{2}{3}e^i \phi \tag{2.10}$$

for $0 \leqslant \phi < 2\pi$ with the semi-infinite line segment

$$-\infty \leqslant u \leqslant -\tfrac{1}{3} \tag{2.11}$$

as shown in figure 1(a). We denote the endpoint (e) of this line segment as $u_e = -\frac{1}{3}$ and the intersection of the circle and the line segment as $u_s = -1$. The solution to (2.9) is shown in figure 2. Since equations (2.8) and (2.9) have real coefficients, the solutions are either real or consist of complex conjugate pairs; this explains why the respective phase diagrams in figures 1(a) and 2 are symmetric about the horizontal axes. Furthermore, under the transformation $u \to 1/u$, the left-hand side of (2.8) retains its form, up to an overall factor; consequently the locus of solutions in figure 1(a) is invariant under this mapping. The analogous statements apply to (2.9) and hence figure 2 concerning the mapping $z \to 1/z$.

The curves in figure 1(a) for the triangular lattice divide the complex u plane into two regions which are complex-temperature extensions of physical phases: (i) the complex ferromagnetic (FM) phase, which is the extension of the physical FM phase occupying the interval $0 \leqslant u \leqslant u_c$, where $u_c = \frac{1}{3}$ is the critical point, and (ii) the complex Z_2-symmetric or paramagnetic (PM) phase, which is the extension of the physical PM phase occupying the interval $u_c < u \leqslant 1$. There is no antiferromagnetically ordered (AFM) phase for complex temperature, just as there was none for physical temperature. Henceforth, for brevity we shall generally drop the qualifier 'complex-temperature extension' on these phases and refer to them simply as FM and PM. As is evident from figure 1(a), there is a section of the line segment (2.11) protruding into the interior of the complex FM phase. The corresponding phase diagrams in the z and v plane are shown in figures 1(b) and (c) (for the latter, see also [11]). Note that the phase labelled 'O' (for 'other') in figures 1(b) and (c) has no overlap with any physical phase.

The complex-temperature phase diagram for the honeycomb lattice is shown in the z plane in figure 2 and consists of FM, AFM and PM phases. As implied by duality, the curves are formally identical to those of the triangular lattice in the v plane (figure 1(c)); however, the actual phase structure is, of course, different. We label the point $z = -1 \equiv z_\ell$ and the intersection points $z = \pm i \equiv z_{s\pm}$. The phase diagram for the hc lattice in the v plane is obtained from figure 1(b) for the t lattice in the z plane by the replacements $z \to v$, FM $\leftrightarrow$ PM, and O $\to$ AFM.

The points on these phase diagrams where curves (including line segments) cross each other are singular points of the curves in the technical terminology of algebraic geometry [20]. Specifically, they are multiple points of index 2, where two arcs of the
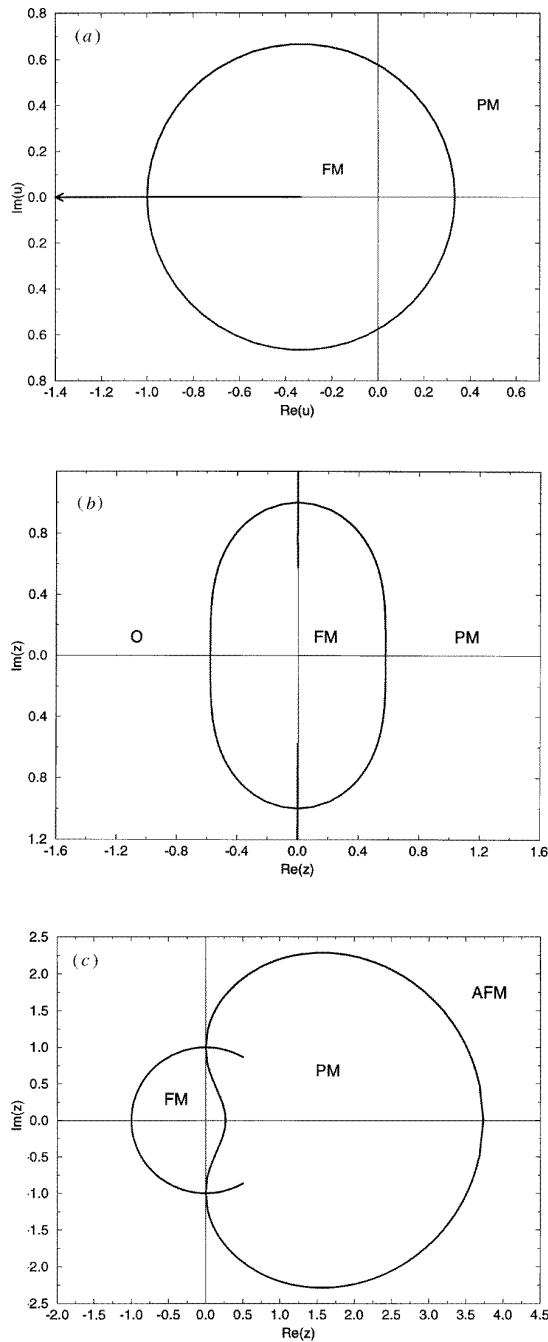
Figure 1. Complex-temperature phases and associated boundaries for the Ising model on the triangular lattice, in the variables (*a*) u, (*b*) z and (*c*) v. See the text for discussion. Note that in (*a*) the line segment extends from $u = -\frac{1}{3}$ to $u = -\infty$, and in (*b*), the two line segments extend, respectively, from $\pm i/\sqrt{3}$ to $\pm i\infty$ along the positive (negative) imaginary axis. In (*c*), the intersections of the curves with the real v axis occur, from left to right, at $v = -1$, $v = v_c = 2 - \sqrt{3}$, and $v = v_c^{-1} = 2 + \sqrt{3}$. The endpoints of the arcs occur at $v = \exp(\pm i\pi/3)$.

curve cross each other (with an angle of $\pi/2$). The arc endpoints at $z = e^{\pm i\pi/3}$ are, of course, also singular points of the curve in the mathematical sense.

Using the general fact that the high-temperature and (for discrete spin models such as the Ising model) the low-temperature expansions have finite radii of convergence, we can use standard analytic continuation arguments to establish that in addition to the free energy
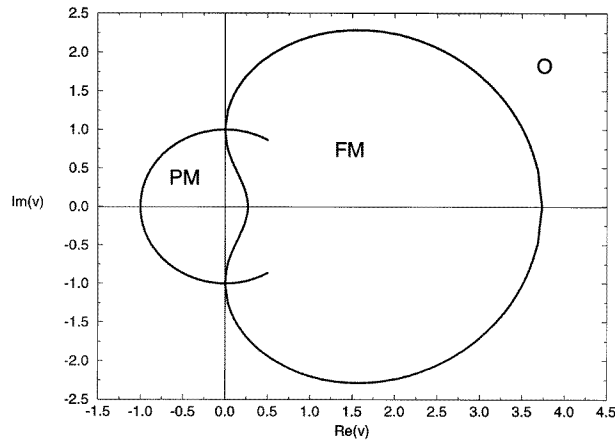
Figure 2. Complex-temperature phases and associated boundaries for the Ising model on the honeycomb lattice, in the variable z. See the text for discussion.

and its derivatives, also the magnetization and susceptibility are analytic functions within each of the complex-temperature phases. This defines these functions as analytic functions of the respective complex variable (u, z or v). Our definition of singular forms of a function at a complex-temperature singular point was given in [9]. Note, in particular, that whereas a physical critical point can only be approached from two different phases, high- or low-temperature, some complex-temperature singular points may be approached from more than two phases.

For the hc lattice we shall also study the staggered susceptibility, $\bar{\chi}^{(a)}$. The low-temperature series for this quantity is expressed in terms of the variable $y = 1/z$, and for our analysis of this series, we observe that the CT phase diagram in the y plane has the same phase boundaries as those in figure 2, owing to the invariance of this boundary under $z \to 1/z$. The phases are, of course, inverted, so that the innermost phase is AFM, to its right, PM, and in the outer region, FM.

Finally, because of the star–triangle relations connecting the Ising model on the triangular and honeycomb lattices, the following exact relations hold [21]:

$$\chi_t(u) = \tfrac{1}{2}\big[\chi_{hc}(z') + \chi_{hc}^{(a)}(z')\big] \tag{2.12}$$

where

$$u = \frac{z'}{1 - z' + z'^2} \tag{2.13}$$

and

$$\chi_t(w) = \tfrac{1}{2}\big[\chi_{hc}(v) + \chi_{hc}^{(a)}(v)\big] = \tfrac{1}{2}\big[\chi_{hc}(v) + \chi_{hc}(-v)\big] \tag{2.14}$$

where

$$v^2 = \frac{w}{1 - w + w^2} \,. \tag{2.15}$$

3. Complex-temperature behaviour of the specific heat

3.1. Triangular lattice

The exact expression for the specific heat C in the FM phase is [15]†

$$k_B^{-1}K^{-2}C = -\frac{8u}{(1-u)^2} + \frac{2(3u^3 + 9u^2 - 7u + 3)k_<}{\pi u^{3/2}(1-u)^2}K(k_<) - \frac{6(1-u)k_<}{\pi u^{3/2}}E(k_<) \tag{3.1}$$

where $K(k) = \int_0^{\pi/2} d\theta[1 - k^2\sin^2\theta]^{-1/2}$ and $E(k) = \int_0^{\pi/2} d\theta[1 - k^2\sin^2\theta]^{1/2}$ are the complete elliptic integrals of the first and second kinds, respectively, and in this subsection we set $k_< \equiv k_{<,t}$. We proceed to analyse the CT singularities of C.

3.1.1. Vicinity of $u = -\frac{1}{3}$. To consider the approach to the point $u = -\frac{1}{3}$ from within the complex extension of the FM phase, we first note that, setting

$$u = -\tfrac{1}{3} + \tfrac{1}{3}\epsilon e^{i\phi} \tag{3.2}$$

where ϵ is real and positive, the elliptic modulus diverges as

$$k_< \to -\frac{i}{2(\epsilon e^{i\phi})^{1/2}} \qquad \text{as} \quad \epsilon \to 0. \tag{3.3}$$

Taking the branch cut for the fractional powers in (2.1) to lie from $u = u_e$ to $u = -\infty$, then for the approach to $u = -\frac{1}{3}$ from the origin along the negative real axis, which corresponds to $\phi = 0$ in (3.2) and (3.3), $k_< \sim -(i/2)(\epsilon)^{-1/2} \to -i\infty$. Next, we let $k_< \equiv i\kappa/\kappa'$, where κ' is the complementary elliptic modulus satisfying $\kappa^2 + \kappa'^2 = 1$. It follows that as $u \to -\frac{1}{3}$, $\kappa = \epsilon/(4+\epsilon) \to 0$. Using the identity [22]

$$K(i\kappa/\kappa') = \kappa'K(\kappa) \tag{3.4}$$

we find that the term involving $K(k_<)$ in (3.1) approaches a constant times $(1 + 3u)^{-1/2}$. In the second term, one factor of $(1 + 3u)^{-1/2}$ comes from the $k_<$ while another comes from the elliptic integral $E(k_<)$, so that this term diverges like $(1 + 3u)^{-1}$. This is the leading divergence in C, so we thus obtain the exact result that as $u \to -\frac{1}{3}$ from within the complex FM phase, the critical exponent for the specific heat is

$$\alpha_e' = 1. \tag{3.5}$$

To our knowledge, this is the first time an algebraic power has been found for the specific heat critical exponent at a singular point in a 2D Ising model. For the critical amplitude, we calculate (taking $\phi = 0$ in (3.2))

$$k_B^{-1}K^{-2}C \to -\frac{2(3)^{3/2}}{\pi}|1 + 3u|^{-1}. \tag{3.6}$$

The infinite set of K values corresponding to the point $u = -\frac{1}{3}$ is

$$K = \frac{1}{4}\ln 3 - \frac{(2n+1)i\pi}{4} \tag{3.7}$$

where $n \in Z$.

† Houtappel's expressions for the internal energy and specific heat, equations (108) and (109), respectively, in [15], are incorrect if one uses the integrals $\epsilon_1(\beta)$ and $\epsilon_2(\beta)$ as he defines them, with the range of integration from $\phi = 0$ to 2π. If, instead, one takes the range of integration from $\phi = 0$ to $\phi = \pi/2$, so that the integrals are just the usual elliptic integrals $K(\sqrt{\beta})$ and $E(\sqrt{\beta})$, then his equations (108) and (109) become correct.

3.1.2. Vicinity of $u = -1$. We first observe that as $u \to -1$ from within the complex FM phase, $k_< \to -1$. It follows that in this case the term involving $E(k_<)$ in (3.1) is finite while the term involving $K(k_<)$ diverges logarithmically, so that at this point $u_s = -1$,

$$\alpha'_s = 0 \quad \text{(log div)}. \tag{3.8}$$

Thus, the divergence in the specific heat at $u = -1$ on the triangular lattice is of the same logarithmic type that it is [8, 9] at $u = -1$ on the square lattice, and the same as it is at the respective physical critical points on both the square and triangular (as well as honeycomb) lattices. For the critical amplitude, using the Taylor series expansion of $k_<$, as a function of u, near $u = -1$,

$$k_< = -1 - 2^{-3}(1 + u)^3 + O((1 + u)^4) \tag{3.9}$$

we calculate

$$k_B^{-1} K^{-2} C \to \frac{12i}{\pi} \ln |1 + u| \qquad \text{as} \quad u \to -1. \tag{3.10}$$

The infinite set of K values corresponding to this point was given in (3.1.8) of paper I: $K = -i\pi/4 + ni\pi/2$ where $n \in Z$.

One can also consider the approach to $u = -1$ from within the complex-temperature extension of the symmetric, PM phase (from the upper left or lower left in figure 1(a)). Using the exact expression for the specific heat applicable in the symmetric phase [15, 19], we find the same logarithmic divergence in C, so that the corresponding exponent is

$$\alpha_s = 0 \quad \text{(log div)}. \tag{3.11}$$

3.2. Honeycomb lattice

From the exact expression (2.7) for f_{hc}, we calculate the specific heat in the FM phase as

$$k_B^{-1} K^{-2} C = -\frac{8z^2}{(1 - z^2)^2} + \frac{[3 - 12(z + z^7) + 28(z^2 + z^6) - 20(z^3 + z^5) + 18z^4]}{\pi(1 + z)(1 - z)^5(1 - z + z^2)} K(k_<)$$
$$- \frac{3(1 - z)(1 + z)}{\pi(1 - z + z^2)} E(k_<) \tag{3.12}$$

(in this subsection we take $k_< \equiv k_{<,hc}$ and $k_> \equiv k_{>,hc}$). The expression (3.12) applies in both the physical FM and AFM phases, and may be analytically continued throughout the respective complex-temperature extensions of these phases.

Since there are singular arc endpoints protruding into the PM phase for the honeycomb lattice (in contrast to the case for the triangular lattice, where there are none), it will be of interest to examine the singular behaviour of various quantities at these endpoints. For this purpose, we observe that in the physical PM phase, one has

$$k_B^{-1} K^{-2} C = v^{-2}(1 - v^2)^{1/2} \left[-\frac{1}{2}(1 - v^2)^{3/2} + \frac{4}{\pi(1 + 3v^2)^{1/2}} K(k_>) - \frac{3(1 - v^2)}{\pi(1 + 3v^2)^{1/2}} E(k_>) \right]. \tag{3.13}$$

3.2.1. Vicinity of $z = -1$. As one approaches the point $z = z_\ell = -1$ from within either the FM or AFM phase, the specific heat diverges, with the dominant divergence arising from the first term in (3.12), which becomes $-2(1 + z)^{-2}$. (There is also a weaker, logarithmic divergence from the term involving $K(k_<)$.) Hence, we find

$$\alpha'_{\ell,\text{FM}} = \alpha'_{\ell,\text{AFM}} = 2. \tag{3.14}$$

Now, $K = -\frac{1}{2}\ln z$, so choosing the branch cut for the complex logarithm to lie along the negative real axis and choosing the first Riemann sheet for the evaluation of the logarithm, as z approaches -1 from above or below the negative real axis, one has $K_\ell = \mp i\pi/2$, respectively, and hence in both cases

$$k_B^{-1}C \to \frac{\pi^2}{2(1+z)^2} \qquad \text{as} \quad z \to -1. \tag{3.15}$$

It is interesting to relate the critical exponent (3.14) to the critical exponent α'_e (3.5) for C on the triangular lattice at the point $u = u_e = -\frac{1}{3}$, which corresponds, via (2.13), to $z' = z = -1$ on the honeycomb lattice. (Recall that although these points correspond to each other, the point $u = -\frac{1}{3}$ in the phase diagram of the triangular lattice can only be approached from within the FM phase, whereas the point $z = -1$ in the phase diagram of the honeycomb lattice can be approached from within either the FM or AFM phases.) Given the star–triangle relations which connect the Ising model on these two lattices and the fact that the Taylor series expansion of $u + \frac{1}{3}$, as a function of z', in the vicinity of $z' = -1$ ($= z$ on the honeycomb lattice), starts with the quadratic term,

$$u + \tfrac{1}{3} = \tfrac{1}{9}(1+z')^2 + \tfrac{1}{9}(1+z')^3 + O((1+z')^4) \tag{3.16}$$

it follows that the exponents $\alpha'_{\ell,\mathrm{FM}} = \alpha'_{\ell,\mathrm{AFM}} = 2$ at $z = -1$ on the honeycomb lattice have twice the value of $\alpha'_e = 1$ at $u = -\frac{1}{3}$ on the triangular lattice.

3.2.2. Vicinity of $z = \pm i$. The points $z = \pm i$ can be approached from within the complex-temperature extensions of the FM, AFM and PM phases. For the approach to $z = \pm i$ from within the complex FM and AFM phases, we find from (3.12) that the first term and the term involving $E(k_<)$ yield finite contributions, while the term involving $K(k_<)$ diverges logarithmically, as $\pm(4i/\pi)K(k_< \to -1)$. Using the fact that as $\lambda \to \pm 1$, $K(\lambda) \to \frac{1}{2}\ln(16/(1-\lambda^2))$, and the Taylor series expansion of $k_<^2$ in the neighbourhood of $z = \pm i$,

$$k_<^2 = 1 - 2(z \mp i)^3 + O((z \mp i)^4) \tag{3.17}$$

we can express the most singular term on the RHS of equation (3.12) as $\mp(2i/\pi)\ln[(z \mp i)^3]$. Evaluating $K = -\frac{1}{2}\ln z$ for $z = \pm i$ on the first Riemann sheet of the logarithm, we have $K = \mp i\pi/4$, so that

$$k_B^{-1}C \sim \pm \frac{i}{8\pi}\ln[(z \mp i)^3]. \tag{3.18}$$

It follows that for $z = z_{s,\pm} = \pm i$,

$$\alpha'_{s,\mathrm{FM}} = \alpha'_{s,\mathrm{AFM}} = 0 \qquad \text{(log div)}. \tag{3.19}$$

The results for $\alpha'_{s,\mathrm{FM}}$ and $\alpha'_{s,\mathrm{AFM}}$ are the same as we found for the analogous exponents on the triangular lattice at the point $u = -1$ corresponding, via (2.13) with $z' \equiv z$, to $z = \pm i$ on the honeycomb lattice.

For the approach to the points $v = v_{s\pm} = \pm i$ from within the PM phase, we find that the term involving $K(k_>)$ produces a logarithmic divergence in C, so that the exponent $\alpha_{s,\mathrm{PM}} \equiv \alpha_s$ is

$$\alpha_s = 0 \quad \text{(log div)}. \tag{3.20}$$

Taking the branch cuts for the factor $(1+3v^2)^{1/2}$ to lie along the semi-infinite line segments from $\pm i/\sqrt{3}$ to $\pm i\infty$, and taking the approach such that $(-1)^{1/2}$ is evaluated as $+i$, we

find that this term yields $(2i/\pi) \ln[(1 - k_>^2)]$. Using the Taylor series expansion of $k_>^2$, as a function of v, near $v = i$,

$$k_>^2 = 1 - 2i(v - i)^3 + O((v - i)^4) \tag{3.21}$$

and its complex conjugate for $v \to -i$, and the result $K = \text{arctanh}(\pm i) = \pm i\pi/4$, we find

$$k_B^{-1} C \sim -\frac{i\pi}{8} \ln[(v \mp i)^3]. \tag{3.22}$$

(In the evaluation of the function $\text{arctanh}(\zeta) = \frac{1}{2} \ln[(1 + \zeta)/(1 - \zeta)]$ here and below, we again use the first Riemann sheet of the logarithm.)

3.2.3. Vicinity of $v = \pm i(3)^{-1/2}$. We next determine the singularities of the specific heat as one approaches the endpoints $v = \pm v_e = \pm i/\sqrt{3}$ of the semi-infinite line segments protruding into the PM phase. We find that C is divergent, with the leading divergence arising from the term involving $E(k_>)$. This term gives $\pm (4\sqrt{3}/\pi)(1 + 3v^2)^{-1}$ as $v \to \pm i$, so

$$\alpha_e = 1. \tag{3.23}$$

Using $K = \text{arctanh}(\pm i/\sqrt{3}) = \pm i\pi/6$, we have

$$k_B^{-1} C \to \mp \frac{\pi}{3^{3/2}(1 + 3v^2)} \qquad \text{as} \quad v \to \pm \frac{i}{\sqrt{3}}. \tag{3.24}$$

3.2.4. Elsewhere on the complex-temperature phase boundary. The free energy f_{hc} is non-analytic across the complex-temperature phase boundaries, and hence, of course, this is also true of its derivatives with respect to K, in particular, the internal energy U and the specific heat C. As an illustration, consider moving along a ray outward from the origin of the z plane defined by $z = re^{i\theta}$ with $\theta < \pi/2$. For a given θ, as r exceeds the critical value $r_c(\theta)$, one passes from the complex-temperature FM phase into the complex-temperature PM phase. At the phase boundary the elliptic modulus $k_<$ has magnitude unity and can be written $k_< = e^{i\phi}$, where the angle ϕ depends on θ. The point $z = z_c$ corresponds to $k_< = 1$, and $z = i$ to $k_< = -1$; ϕ increases from 0 at $\theta = 0$ to π at $\theta = \pi/2$. Hence, for $0 < \theta < \pi/2$, $k_<$ has a non-zero imaginary part. Now when one passes through the FM–PM phase boundary along the ray at this angle θ, one changes the argument of the elliptic integrals from $k_< = e^{i\phi}$ to $k_> = 1/k_< = e^{-i\phi}$. The elliptic integrals $K(k)$ and $E(k)$ are analytic functions of k^2 with, respectively, a logarithmically divergent and a finite branch point singularity at $k^2 = 1$ and associated branch cuts which may be taken to lie along the positive real axis in the k^2 plane. In particular, $K(k)$ and $E(k)$ are both analytic at the point $k = k_< = e^{i\phi}$ for $0 < \theta < \pi/2$. Hence, when we replace the argument $k_<$ by $k_>$, which is the complex conjugate of $k_<$ on the unit circle, we have $F(k_> = e^{-i\phi}) = F(k_< = e^{i\phi})^*$ for $F = K, E$. Since these elliptic integrals are complex for generic complex $k_<$, it follows that their imaginary part is discontinuous across the FM–PM boundary. The coefficients of the elliptic integrals are also different functions in the FM and PM phases, and these coefficients are discontinuous as one crosses the boundary between these phases on the above ray. Combining these, we find that the specific heat itself is discontinuous as one moves across the FM–PM boundary on this ray. A similar discussion applies to the specific heat on the triangular lattice.

4. Complex-temperature behaviour of the spontaneous magnetization

4.1. General

For the $\Lambda = $ sq, t, and hc lattices, M is given by

$$M = \left(1 - (k_{<,\Lambda})^2\right)^{1/8}. \tag{4.1}$$

From equations (2.1) and (2.2), one has [17]

$$M_{\mathrm{t}} = \left(\frac{1+u}{1-u}\right)^{3/8}\left(\frac{1-3u}{1+3u}\right)^{1/8} \tag{4.2}$$

and [18]

$$M_{\mathrm{hc}} = \frac{(1+z^2)^{3/8}(1-4z+z^2)^{1/8}}{(1-z)^{3/4}(1+z)^{1/4}}. \tag{4.3}$$

(Here, $(1-4z+z^2) = (1-z/z_{\mathrm{c}})(1-z_{\mathrm{c}}z)$, where $z_{\mathrm{c}} = 2-\sqrt{3}$ is the physical critical point for the honeycomb lattice.) These expressions apply within the respective physical FM phases on these two lattices and, by analytic continuation, throughout the complex-temperature extension of these phases, with $M = 0$ elsewhere. We recall that, as a consequence of the star–triangle relation which connects the Ising model on the triangular and honeycomb lattices [19],

$$M_{\mathrm{t}}(u) = M_{\mathrm{hc}}(z') \tag{4.4}$$

where u and z' are related by (2.13).

Concerning the singular points of the magnetization, in addition to its well known continuous zero at the physical critical point $u_{\mathrm{c}} = \frac{1}{3}$ on the triangular lattice (with exponent $\beta = \frac{1}{8}$), M_{t} also vanishes at the complex-temperature singular point $u = -1 \equiv u_{\mathrm{s}}$, with exponent

$$\beta_{\mathrm{s}} = \frac{3}{8}. \tag{4.5}$$

With the exception of these two points, u_{c} and u_{s}, M_{t} vanishes discontinuously elsewhere along the outer boundary of the complex-temperature extension of the FM phase. In addition, M_{t} diverges at the CT point $u = u_{\mathrm{e}} = -\frac{1}{3}$, with exponent

$$\beta_{\mathrm{e}} = -\frac{1}{8}. \tag{4.6}$$

Note that despite the $(1-u)^{-3/8}$ factor in the exact expression (4.2), M_{t} does not in fact diverge at $u = 1$, since this point lies outside the FM phase where equation (4.2) applies (indeed, M_{t} is identically zero in the vicinity of this point $z = 1$, which is in the PM phase). Similarly, in addition to its well known continuous zero at the physical critical point $z_{\mathrm{c}} = 2 - \sqrt{3}$ on the honeycomb lattice (with exponent $\beta = \frac{1}{8}$), M_{hc} vanishes continuously at the complex-temperature points $z = z_{s\pm} = \pm i$, with exponent $\beta_{\mathrm{s}} = \frac{3}{8}$. The fact that this exponent is the same as the exponent with which M_{t} vanishes at $u_{\mathrm{s}} = -1$ follows from (4.4), given the fact that $u = -1$ on the triangular lattice corresponds, via equation (2.13), to $z' = z = \pm i$ on the honeycomb lattice. Elsewhere along the boundary of the FM phase, M_{hc} vanishes discontinuously. Finally, M_{hc} has a divergence at $z = z_{\ell} = -1$, with exponent

$$\beta_{\ell} = -\frac{1}{4}. \tag{4.7}$$

Note that the apparent zero at $z = 1/z_{\mathrm{c}}$ and the apparent divergence at $z = 1$ do not actually occur, since these points are outside the FM phase where (4.3) applies. The fact that the exponent β_{ℓ} with which M_{hc} diverges at the point $z = -1$ on the honeycomb lattice is

twice the exponent β_e with which M_t diverges at the point $u = -\frac{1}{3}$ on the triangular lattice (which corresponds to $z' = z = -1$ via (2.13)) follows from (4.4) and the property that the Taylor series expansion of $u + \frac{1}{3}$, as a function of z', in the vicinity of $z' = -1$, starts with the quadratic term, as given in (3.16).

Since the honeycomb lattice is loose-packed, one immediately infers the staggered magnetization $M_{hc,st}$ from the (uniform) magnetization M_{hc}: formally,

$$M_{hc,st}(y) = M_{hc}(z \to y) \tag{4.8}$$

where $y = 1/z$.

4.2. Theorem on $M \to \infty \Rightarrow \chi \to \infty$

Such an exotic phenomenon as a divergent spontaneous magnetization, as occurs for M_t at $u = -\frac{1}{3}$, has received very little attention in the literature. Indeed, one is used to regarding the divergence in the susceptibility at the physical critical point as a reflection of the fact that $M = 0$ there but is just on the verge of becoming non-zero, so that an arbitrarily small external field has an arbitrarily large effect. This intuitive physical understanding does not prepare one to deal with the case when M diverges and the question of how the susceptibility behaves at such a point. We begin by stating and proving a theorem which deals with an important effect of such a divergence. First, we prove a lemma concerning two-spin correlation functions:

Lemma 1. Assume that a given statistical mechanical model has a phase with ferromagnetic long-range order. In this phase, and in its extension to complex temperature, the two-spin correlation function can always be written in the form

$$\langle \sigma_n \sigma_{n'} \rangle = M^2 c(n, n') \tag{4.9}$$

where M is the spontaneous magnetization and $c(n, n')$ contains all of the dependence on the lattice sites n and n'.

Proof. This result follows easily from the fact that one of the equivalent definitions of M is precisely via the relation

$$M^2 = \lim_{|n-n'| \to \infty} \langle \sigma_n \sigma_{n'} \rangle. \tag{4.10}$$

Given the correlation function $\langle \sigma_n \sigma_{n'} \rangle$, one may thus calculate M^2 from the limit (4.10) and divide, thereby obtaining the function $c(n, n')$ (with the property $\lim_{|n-n'| \to \infty} c(n, n') = 1$). $\square$

As an immediate corollary, we have

Lemma 2. Assume that a given statistical mechanical model has a phase with ferromagnetic long-range order. In this phase, and in its extension to complex temperature, the connected two-spin correlation function can always be written in the form

$$\langle \sigma_n \sigma_{n'} \rangle_{conn} = M^2 c(n, n')_{conn} \tag{4.11}$$

where M is the spontaneous magnetization and $c(n, n')_{conn}$ contains all of the dependence on the lattice sites n and n'.

Proof. This follows immediately from the definition of the connected two-spin correlation function as $\langle \sigma_n \sigma_{n'} \rangle_{conn} \equiv \langle \sigma_n \sigma_{n'} \rangle - M^2$, which also shows that $c(n, n')_{conn} = c(n, n') - 1$. $\square$

We then proceed to

Theorem 1. If the magnetization M diverges as one approaches a given point from within the (complex-temperature extension of the) ferromagnetic phase, then, in the same limit, the susceptibility also diverges.

Proof. The susceptibility $\bar{\chi}$ is given as the sum over the connected two-spin correlation functions

$$\bar{\chi} = N_s^{-1} \lim_{N_s \to \infty} \sum_{n,n'} \langle \sigma_n \sigma_{n'} \rangle_{\text{conn}}$$

$$= \sum_n \langle \sigma_0 \sigma_n \rangle_{\text{conn}} \tag{4.12}$$

(where the homogeneity of the lattice has been used in the second line). Using lemma 2, we have

$$\bar{\chi} = M^2 \sum_n c(n, n')_{\text{conn}} . \tag{4.13}$$

It follows that, in general, a divergence in M will cause a divergence in $\bar{\chi}$.   □

Note that this would be true even in the hypothetical case in which M is divergent but the correlation length is finite, so that the sum $\sum_n c(n, n')_{\text{conn}}$ converges.

We next apply theorem 1 to the current study:

Corollary 1. For the Ising model on the triangular lattice, $\bar{\chi}_t$ has a divergent singularity at $u = -\frac{1}{3}$.

Proof. This follows from the fact that, as we know from the exact result, (4.2), M_t diverges at $u = -\frac{1}{3}$ together with theorem 1.   □

Note that unlike the study of the low-temperature series, which is, of course, approximate since the series only extends to finite order, this is an exact rigorous result. What the studies by Guttmann [6] and the present authors yield beyond the result of the theorem is the actual values of the exponent γ_e' and critical amplitude A_e'.

Also, observe that we did not explicitly use any property of the correlation length to make this conclusion. Our theorem and corollary allow us to infer without a direct calculation that the correlation length does in fact diverge at $u = -\frac{1}{3}$ (as this point is approached from the interior of the complex-temperature extension of the FM phase, i.e. from all directions except from the left along the singular line segment (2.11)). We can deduce this because if the correlation length were finite, then the sum over two-spin correlation functions in (4.12) would be finite. (Since only the large-distance behaviour is relevant to a possible divergence, one can replace the sum by an integral, and because of the exponential damping from $\langle \sigma_0 \sigma_r \rangle \sim r^{-p} e^{r/\xi}$, the integral is finite.) But then since the only divergence would arise from the prefactor of M_t^2, we would have the exponent relation $\gamma_e' = -2\beta_e$. Since $-2\beta_e = \frac{1}{4}$, while the series analyses yield $\gamma_e' = \frac{5}{4}$, the above exponent relation does not hold. This shows then, that the correlation length diverges at $u = -\frac{1}{3}$.

5. Analysis of low-temperature susceptibility series

5.1. General

Here we shall study the complex-temperature singularities of the susceptibility $\bar{\chi}$ which occur as one approaches the boundary of the (complex-temperature extension of the)

FM phase from within this phase, for the triangular and honeycomb lattices. The low-temperature series expansion for $\bar{\chi}_t$ is given by

$$\bar{\chi}_t = 4u^3 \left(1 + \sum_{n=1}^{\infty} c_{n,t} u^n \right). \tag{5.1}$$

The analogous series expansion for $\bar{\chi}_{hc}$ on the honeycomb lattice is of the same form, with u replaced by z and $c_{n,t}$ by $c_{n,hc}$. We shall also study the staggered susceptibility, $\bar{\chi}_{hc}^{(a)}$, which has a low-temperature series similar to that for $\bar{\chi}_{hc}$ with z replaced by $y = 1/z$, the expansion variable in the AFM phase, and $c_{n,hc}$ replaced by $c_{n,hc}^{(a)}$. These three series are related by (2.12). They each have finite radii of convergence and, by analytic continuation from the respective physical low-temperature intervals: (i) $0 \leqslant u < u_c$, (ii) $0 \leqslant z < z_c$ and (iii) $0 \leqslant y < y_c$, apply throughout the complex extension of the FM phases on the t and hc lattices and, in the third case, the AFM phase on the hc lattice. (Here y_c is the critical point separating the PM and AFM phases on the hc lattice, which occurs at $z = 1/z_c = 2 + \sqrt{3}$, so that $y_c = 2 - \sqrt{3}$, the same numerical value as the critical point z_c separating the PM and FM phases.) Since the respective u^3, z^3 and y^3 prefactors are known exactly, it is convenient to study the remaining factors $\bar{\chi}_{r,t} = u^{-3} \bar{\chi}_t$, $\bar{\chi}_{r,hc} = z^{-3} \bar{\chi}_{hc}$, and $\bar{\chi}_{r,hc}^{(a)} = y^{-3} \bar{\chi}_{hc}^{(a)}$. Following earlier work [23], the expansion coefficients $c_{n,t}$, $c_{n,hc}$, and $c_{n,hc}^{(a)}$ were calculated by the King's College group to order $n = 13$ (i.e. $\bar{\chi}_t$, $\bar{\chi}_{hc}$, and $\bar{\chi}_{hc}^{(a)}$ to $O(u^{16})$, $O(z^{16})$ and $O(y^{16})$, respectively) in 1971 [24], and to order $n = 18$ in 1975 [25]. We have checked and found that apparently these series have not been calculated to higher order subsequently [26, 27].

As one approaches a generic complex singular point denoted ζ_{sing} (where $\zeta = u$ and z for the t and hc lattices, respectively) from within the complex-temperature extension of the FM phase, $\bar{\chi}$ is assumed to have the leading singularity

$$\bar{\chi}(\zeta) \sim A'_{sing} (1 - \zeta/\zeta_{sing})^{-\gamma'_{sing}} (1 + a_1(1 - \zeta/\zeta_{sing}) + \cdots) \tag{5.2}$$

where A'_{sing} and γ'_{sing} denote the critical amplitude and the corresponding critical exponent, and the ... represent analytic confluent corrections. One may observe that we have not included non-analytic confluent corrections to the scaling form in (5.2). The reason is that, although such terms are generally present at critical points in statistical mechanical models, previous studies have indicated that they are very weak or absent for the usual critical point of the 2D Ising model [28, 29].

5.2. Triangular lattice

It was noticed quite early that the low-temperature series for $\bar{\chi}_t$ does not give very good results for the position of the physical critical point or for its exponent γ'. The cause for this was recognized to be the existence of the unphysical, complex-temperature singularity at $u_e = -\frac{1}{3}$, the same distance from the origin (on the opposite side) as the physical singularity at u_c [4, 5]. A study of the CT singularity in $\bar{\chi}_t$ at u_e was carried out by Guttmann using ratio and d log Padé methods. Writing the singular form as $\bar{\chi}_t \simeq A'_e (1 - u/u_e)^{-\gamma'_e}$, he obtained

$$\gamma'_e = \tfrac{5}{4} \qquad A'_e = -0.0568 \pm 0.0008. \tag{5.3}$$

We have extended this work with the use of differential approximants (DAs; for a review, see [30]), and have compared these with results from d log Padé approximants (PAs). We have found that the DAs yield a considerably more precise determination of the exponent than the d log PAs. Given the evidence that non-analytic confluent singularities are weak or absent for the physical critical point, which motivates the form (5.2), $K = 1$ differential approximants should be sufficient for our purposes here. We have performed the analysis

Table 1. Values of $r_e \equiv |\tilde{u}_{sing} - \tilde{u}_e|/|\tilde{u}_e|$ (where $\tilde{u}_e = -\frac{1}{6}$) and γ_e' from differential approximants to low-temperature series for $\bar{\chi}_{r,t}(\tilde{u})$. We only display entries which satisfy the accuracy criterion $r_e \leqslant 1 \times 10^{-4}$.

$[L/M_0; M_1]$	$10^4 r_e$	γ_e'	$[L/M_0; M_1]$	$10^4 r_e$	γ_e'
[0/6; 7]	0.56	1.2516	[3/5; 6]	0.68	1.2545
[0/6; 8]	0.01	1.2481	[3/5; 7]	0.44	1.2446
[0/7; 6]	0.56	1.2517	[3/6; 5]	0.68	1.2545
[0/7; 7]	0.14	1.2471	[3/6; 6]	0.61	1.2431
[0/7; 8]	0.27	1.2462	[3/6; 7]	0.31	1.2458
[0/7; 9]	0.23	1.2466	[3/7; 5]	0.44	1.2446
[0/8; 6]	0.0049	1.2481	[3/7; 6]	0.31	1.2458
[0/8; 7]	0.27	1.2462	[4/5; 5]	0.49	1.2528
[0/8; 8]	0.23	1.2466	[4/5; 6]	0.55	1.2436
[0/9; 7]	0.23	1.2466	[4/5; 7]	0.21	1.2468
[1/6; 6]	0.74	1.2424	[4/6; 5]	0.55	1.2436
[1/6; 7]	0.48	1.2443	[4/6; 6]	0.44	1.2444
[1/6; 8]	0.50	1.2441	[4/7; 5]	0.20	1.2469
[1/7; 6]	0.48	1.2443	[5/5; 5]	0.54	1.2437
[1/7; 7]	0.51	1.2440	[5/5; 6]	0.19	1.2470
[1/7; 8]	0.49	1.2535	[5/6; 4]	0.85	1.2573
[1/8; 6]	0.50	1.2441	[5/6; 5]	0.18	1.2472
[1/8; 7]	0.49	1.2535	[6/4; 6]	0.29	1.2458
[2/5; 7]	0.90	1.2564	[6/5; 3]	1.0	1.2594
[2/6; 6]	0.45	1.2524	[6/5; 5]	0.22	1.2467
[2/6; 7]	0.54	1.2438	[6/6; 4]	0.032	1.2496
[2/6; 8]	0.22	1.2467	[7/4; 5]	0.43	1.2444
[2/7; 5]	0.90	1.2565	[7/5; 4]	0.15	1.2507
[2/7; 6]	0.54	1.2438	[8/5; 3]	0.87	1.2578
[2/7; 7]	0.28	1.2461			
[2/8; 6]	0.22	1.2467			

both on the series for $\bar{\chi}_t$ in the variable u and in a transformed variable $\tilde{u} = u/(1 - 3u)$, which has the effect of mapping the physical singularity at $u_c = \frac{1}{3}$ to infinity and thereby increasing the sensitivity to the CT singularity at $u = -\frac{1}{3}$, or equivalently, $\tilde{u} = -\frac{1}{6}$. As expected, our most precise results were obtained with this transformed series; these are shown in table 1.

The results of this study agree with the old inference of a singularity in $\bar{\chi}$ at $u = u_e = -\frac{1}{3}$ [5]. For the exponent, we obtain

$$\gamma_e' = 1.249 \pm 0.005 \tag{5.4}$$

strongly supporting the conclusion that the exact value is $\gamma_e' = \frac{5}{4}$, in excellent agreement with Guttmann's previous inference of this value using ratio and d log Padé methods [6].

For the critical amplitude A_e', we have used a method complementary to [6]: we compute the series for $(\bar{\chi}_{r,t})^{1/\gamma_e'}$. Since the exact function $(\bar{\chi}_{r,t})^{1/\gamma_e'}$ has a simple pole at u_e, one performs a Padé analysis on the series itself instead of its logarithmic derivative. The residue at this pole is $R_e = -u_e(A_{r,e}')^{1/\gamma_e'}$, where $A_{r,e}'$ denotes the critical amplitude for $\bar{\chi}_r$. It follows that $A_e' = 4u_e^3 A_{r,e}' = -4(3)^{-7/4} R_e^{5/4}$. Using the inferred value $\gamma_e' = \frac{5}{4}$ to compute the series, we obtain $A_e' = 2^{5/4} \tilde{A}_e'$, and hence

$$A_e' = -0.057\,66 \pm 0.000\,15 \tag{5.5}$$

which is in agreement with [6] and has a somewhat smaller estimated uncertainty.

It is of interest to compare this with the critical amplitude at the physical critical point, as approached from within the FM phase. For reference, we note that many authors express the singularity in terms of T rather than u, namely, $\bar{\chi}_{\text{sing}} \sim A'_{\text{c},T}(1 - T/T_{\text{c}})^{-\gamma'} \sim A'_{\text{c}}(1 - u/u_{\text{c}})^{-\gamma'}$ with $\gamma' = \frac{7}{4}$. The critical amplitudes are related according to $A'_{\text{c}} = (4K_{\text{c}})^{7/4} A'_{\text{c},T}$. After early work by Essam and Fisher [31], Guttmann used a low-temperature series analysis to obtain $A'_{\text{c},T} = 0.0246 \pm 0.0002$, i.e. $A_{\text{c}} = 0.0290 \pm 0.0002$ and analytic methods to obtain the high-precision result $A'_{\text{c},T} = 0.024\,518\,9020$, i.e. $A'_{\text{c}} = 0.028\,905\,388$ [32] (see also [33, 34]). Using this latter value, we find

$$\frac{A'_{\text{e}}}{A'_{\text{c}}} = -(1.995 \pm 0.005) \tag{5.6}$$

where the uncertainty arises completely from the uncertainty in A'_{e}. The ratio (5.6) is slightly less than, but close to, the simple relation $A'_{\text{e}}/A'_{\text{c}} = -2$.

We have also carried out an analysis of the low-temperature series for $\bar{\chi}_{\text{t}}$ (again with d log Padé and differential approximants) to study the singularity at $u = -1$. However, we have found that the series, at least at the order to which it has been calculated, cannot probe this point very sensitively. We believe that the reason for this is the fact that the series is dominated by the singularity at $u = -\frac{1}{3}$, which is not only closer to the origin but also directly in front of the point $u = -1$ as approached from the origin. (For further details, the reader may consult our file hep-lat/9411023.) We can say that if the scaling relation $\alpha' + 2\beta + \gamma' = 2$ holds at $u = -1$ for the Ising model on the triangular lattice, as it does on the square lattice, then, given the exact result that $\beta_{\text{s}} = \frac{3}{8}$ (see equation (4.2) below) and our finding that $\alpha'_{\text{s}} = 0$ from the exact free energy (see equation (3.8) below), it would follow that $\gamma'_{\text{s}} = \frac{5}{4}$, which would be equal to the value of the exponent γ'_{s} for the singularity at u_{e}.

5.3. Honeycomb lattice

5.3.1. Singularity at $z = -1 \equiv z_\ell$. Here we study the singularities in $\bar{\chi}_{\text{hc}}$ and $\bar{\chi}_{\text{hc}}^{(a)}$ as one approaches the point $z_\ell = -1$ from within the FM and AFM phases. (For brevity of notation, we sometimes omit the subscript hc.) Before proceeding, we consider the implications of the exact relation (2.12). Given that $\chi_{\text{t}}(u)$ has a singularity at $u = u_{\text{e}} = -\frac{1}{3}$, it follows that the sum $\chi_{\text{hc}}(z') + \chi_{\text{hc}}^{(a)}(z')$ on the honeycomb lattice has the same singularity at the point $z' = 1$ corresponding via (2.13) to $u = -\frac{1}{3}$. But this does not, by itself, determine the singularities in the individual functions χ_{hc} and $\chi_{\text{hc}}^{(a)}$ at this point. If one could prove that both χ_{hc} and $\chi_{\text{hc}}^{(a)}$ necessarily have the same singularity at $z' = -1$, then the relation (2.12), together with the result that $\chi_{\text{t}}(u) \sim (1 + 3u)^{-\gamma'_{\text{e}}}$ with $\gamma'_{\text{e}} = \frac{5}{4}$, the Taylor series expansion of $u + \frac{1}{3}$ as a function of z' (i.e. z on the honeycomb lattice) in the vicinity of $z' = -1$, equation (3.16), would imply that $\gamma'_\ell = \gamma'_{\ell,a} = 2\gamma'_{\text{e}} = \frac{5}{2}$. However, although it is plausible that χ_{hc} and $\chi_{\text{hc}}^{(a)}$ do have the same singularities at $z = -1$, there is no simple relationship between the respective low-temperature series for these two functions, as is clear from the first few terms [24],

$$\bar{\chi} = 4z^3\left[1 + 6z + 27z^2 + 122z^3 + 516z^4 + 2148z^5 + \cdots\right] \tag{5.7}$$

and

$$\bar{\chi}^{(a)} = 4y^3\left[1 + 0 \cdot y + 3y^2 + 2y^3 + 12y^4 + 24y^5 + \cdots\right]. \tag{5.8}$$

Hence, an explicit series analysis is worthwhile to obtain the critical exponents.

Table 2. Values of $r_\ell \equiv |z_{\text{sing}} - z_\ell|/|z_\ell|$ (where $z_\ell = -1$) and γ'_ℓ from differential approximants to low-temperature series for $\bar{\chi}_{r,\text{hc}}(z)$. We only display entries which satisfy the accuracy criterion $r_\ell \leqslant 10^{-2}$.

$[L/M_0; M_1]$	$10^2 r_\ell$	γ'_ℓ	$[L/M_0; M_1]$	$10^2 r_\ell$	γ'_ℓ
$[1/6; 6]$	0.96	2.5188	$[3/6; 7]$	0.41	2.4136
$[1/6; 7]$	0.009	2.3989	$[3/7; 6]$	0.96	2.3022
$[1/7; 5]$	0.57	2.4418	$[4/4; 6]$	0.51	2.1301
$[2/6; 6]$	0.48	2.4588	$[4/6; 6]$	0.54	2.3580
$[2/7; 5]$	0.54	2.2967	$[5/4; 5]$	0.007	2.1252
			$[5/4; 6]$	0.65	2.0704

5.3.2. Exponent at $z = -1$.   Since we obtained more precise results from the DA than the d log PA study, we concentrate on the former here. As we did for our work on the square and triangular lattice, we use an extrapolation technique in which we plot the value of the exponent obtained from each differential approximant as a function of the distance of the corresponding pole location from the inferred exact position of the singularity and then extrapolate to zero distance of the pole from this singularity to obtain the estimate of the exponent. Of course, this is essentially equivalent to using biased differential approximants. We present our results in table 2.

   These results yield evidence that $\bar{\chi}_{\text{hc}}$ has a divergent singularity at $z = -1$, as one approaches this point from the complex-temperature FM phase. Since the values of the exponent from the differential approximants show considerable scatter, it is only possible to extract a rather crude estimate for γ'_ℓ. We obtain

$$\gamma'_\ell = 2.4 \pm 0.3. \tag{5.9}$$

This is consistent with the following inference which we shall make for the exact value of this exponent:

$$\gamma'_\ell = \tfrac{5}{2}. \tag{5.10}$$

5.3.3. Critical exponent of $\bar{\chi}_{\text{hc}}^{(a)}$ at the $z = -1$ singularity.   The staggered susceptibility $\bar{\chi}_{\text{hc}}^{(a)}$ has a well known divergent singularity at $y = y_c = 2 - \sqrt{3}$ with low-temperature exponent $\gamma^{(a)'} = \tfrac{7}{4}$. Here we analyse the complex-temperature singularities of this function using its low-temperature series. Our results from the differential approximants are listed in table 3. From these we find strong evidence that as one approaches the point $y = 1/z = -1$ from within the complex AFM phase, $\bar{\chi}_{\text{hc}}^{(a)}$ has a divergent singularity. It is interesting that the exponent values from these differential approximants show less scatter than those which we found for the uniform susceptibility. Using our extrapolation technique, we obtain

$$\gamma'_{\ell,a} = 2.50 \pm 0.03 \tag{5.11}$$

where the quoted uncertainty is a subjective estimate of the accuracy of the extrapolation. This is consistent with the following exact value, which we infer:

$$\gamma'_{\ell,a} = \tfrac{5}{2} \tag{5.12}$$

so that, with this inference,

$$\gamma'_{\ell,a} = \gamma'_\ell. \tag{5.13}$$

Table 3. Values of $r_y = |y_{\text{sing}} - y_\ell|/|y_\ell|$ (where $y_\ell = -1$) and $\gamma'_{\ell,a}$ from differential approximants to low-temperature series for $\bar{\chi}^{(a)}_{r,\text{hc}}(y)$. We only display entries which satisfy the accuracy criterion $r_y \leqslant 10^{-2}$.

$[L/M_0; M_1]$	$10^2 r_y$	$\gamma'_{\ell,a}$	$[L/M_0; M_1]$	$10^2 r_y$	$\gamma'_{\ell,a}$
[0/7; 6]	0.12	2.4468	[2/7; 6]	0.40	2.4265
[0/7; 7]	0.98	2.3222	[2/8; 6]	0.008	2.4837
[0/7; 8]	0.065	2.4810	[3/6; 4]	1.0	2.7256
[0/7; 9]	0.36	2.5718	[3/6; 5]	0.42	2.6064
[0/8; 7]	0.48	2.3996	[3/6; 6]	0.39	2.4283
[0/9; 7]	0.15	2.5192	[3/6; 7]	0.29	2.5645
[1/6; 7]	0.47	2.4076	[3/7; 6]	0.014	2.4976
[1/6; 8]	0.13	2.5237	[4/6; 4]	0.36	2.6153
[1/7; 6]	0.75	2.3586	[4/6; 5]	0.83	2.5168
[1/8; 6]	0.12	2.4668	[4/6; 6]	0.16	2.4518
[2/5; 7]	0.74	2.3391	[5/4; 6]	0.96	2.4347
[2/6; 6]	0.42	2.4235	[5/5; 6]	0.046	2.4251
[2/6; 7]	0.41	2.4243	[5/6; 4]	0.68	2.4105
[2/6; 8]	0.31	2.5572	[5/6; 5]	0.24	2.4589
[2/7; 5]	0.18	2.5643			

We have also calculated the critical amplitude $A'_{\ell,a}$ in the staggered susceptibility as one approaches $z = y = -1$ from the complex AFM phase, using the same methods as those we used for the triangular lattice. We find

$$A'_{\ell,a} = -0.700 \pm 0.010\,. \tag{5.14}$$

Having inferred that $\bar{\chi}_{\text{hc}}$ and $\bar{\chi}^{(a)}_{\text{hc}}$ have the same power-law divergence at $z = y = -1$, as approached from the complex FM and AFM phases, respectively, we can next use the relation (2.12) to compute A'_ℓ. For this purpose, we recall that on the triangular lattice, at the corresponding point $u = u_e = -\frac{1}{3}$, the (uniform) susceptibility $\bar{\chi}_t$ has the leading singularity $\bar{\chi}_t \sim A'_{e,t}(1 + 3u)^{-5/4}$. Using this, together with the Taylor series expansion (3.16), we find the following relations among the critical amplitude $A'_{e,t}$ at $u = -\frac{1}{3}$ on the triangular lattice and A'_ℓ and $A'_{\ell,a}$ at $z = -1$ on the honeycomb lattice:

$$2(3^{5/4})A'_{e,t} = A'_\ell + A'_{\ell,a}\,. \tag{5.15}$$

Substituting (5.14) and (5.5) into (2.12), we obtain the critical amplitude for the uniform susceptibility,

$$A'_\ell = 0.245 \pm 0.010\,. \tag{5.16}$$

We also used the low-temperature series for $\bar{\chi}_{\text{hc}}$ and $\bar{\chi}^{(a)}_{\text{hc}}$ to investigate the singular behaviour of these functions as one approaches the points $z = z_{s\pm} = \pm i$ from within the complex-temperature FM and AFM phases, respectively. However, we were not able to obtain conclusive results.

6. Some remarks on exponent relations

We have previously shown that in general at complex temperature singularities, a number of the usual scaling relations applicable for physical critical points do not hold [7, 9]. We have demonstrated that at $u = u_s = -1$ on the square lattice, first $\gamma_s \neq \gamma'_s$, and second, there is a violation of universality, as evidenced by the lattice dependence of the

magnetization critical exponent β. Third, as one approaches the point $u = -1$ from within the complex-temperature FM phase, the inverse correlation length $\xi_{\mathrm{FM,row}}^{-1}$ defined from the row (or equivalently, column) connected two-spin correlation functions (analytically continued throughout the complex-temperature extension of the FM phase) vanishes like $|1+u|^{\nu'_s}$ with $\nu'_s = 1$, whereas the inverse correlation length $\xi_{\mathrm{FM},d}^{-1}$ defined from the diagonal connected two-spin correlation functions vanishes like $|1 + u|^{-\nu_{s,\mathrm{diag}}}$ with $\nu_{s,\mathrm{diag}} = 2$ in the same limit [9]. We have generalized this as follows. The exact calculation of the asymptotic form of the two-spin correlation function $\langle \sigma_{0,0} \sigma_{m,n} \rangle$ [35] for the square lattice (analytically continued throughout the complex FM phase), we have shown that the inverse correlation length extracted from $\langle \sigma_{0,0} \sigma_{m,n} \rangle_{\mathrm{conn}}$ as $r = (m^2 + n^2)^{1/2} \to \infty$ vanishes as $u \to u_s$ from within the complex FM phase like $|u + 1|^{\nu'_s}$ with $\nu'_s = 1$ if $\theta = \arctan(m/n)$ does not represent a diagonal of the lattice, i.e. is not equal to $\pm \pi/2$ or $\pm 3\pi/2$. This result in turn undermines the naive use of renormalization-group methods to derive scaling relations for exponents since these methods rely on the existence of a single diverging length scale provided by the correlation length. These findings show that universality, scaling, and exponent relations which were applicable to physical critical points do not, in general, hold for complex-temperature singular points.

For the singularity at $u = -1$ on the triangular lattice, the exact results (3.8) and (4.5), together with the value $\gamma'_s = \frac{5}{4}$ inferred from series analysis [6], imply that the exponent relation $\alpha'_s + 2\beta_s + \gamma'_s = 2$ is satisfied as this point is approached from within the FM phase. The same relation is also satisfied for the approach to $u = -1$ from the FM phase on the square lattice, given the exact values $\alpha'_s = 0$ (log div), $\beta_s = \frac{1}{4}$, and the value $\gamma'_s = \frac{3}{2}$ inferred from series analyses [8, 9] and from an exact exponent relation $\gamma'_s = 2(\gamma - 1)$ [9, 36]. However, the analogous relation for the approach to $u = -1$ from within the symmetric phase, namely $\alpha_s + 2\beta_s + \gamma_s = 2$, is false, since $\alpha_s = 0$ (log divergence) and [7] $\gamma_s < 0$.

Concerning exponent relations at the singularity $z = -1$ on the honeycomb lattice, using the exact values $\alpha'_{\ell,\mathrm{FM}} = 2$ from equation (3.14) and $\beta_\ell = -\frac{1}{4}$ from (4.7) and our inferred exact value from series analysis, $\gamma'_{\ell,\mathrm{FM}} = \frac{5}{2}$, we find that

$$\alpha'_{\ell,\mathrm{FM}} + 2\beta_\ell + \gamma'_{\ell,\mathrm{FM}} = 4. \qquad (6.1)$$

(More generally, using our actual numerical determination of $\gamma'_{\ell,\mathrm{FM}}$ in equation (5.9), the right-hand side of the equation is consistent with being equal to 4.) The right-hand side of (6.1) is twice the value at physical critical points. We have given an explanation above of why the exponents $\alpha'_{\ell,\mathrm{FM}}$ and β_ℓ for the singularity at $z = -1$ on the honeycomb lattice have twice the values of the respective exponents α'_e and β_e on the triangular lattice, at the point $u = -\frac{1}{3}$ which corresponds, via (2.13) to $z' = z = -1$ on the honeycomb lattice; this followed from the star–triangle relation connecting the Ising model on these two lattices together with the fact that the Taylor series expansion of $u + \frac{1}{3}$, as a function of z', starts at quadratic order. We have also noted above the connection of our finding from the series analysis that γ'_ℓ for the honeycomb lattice has twice the value of the corresponding γ' exponent for the singularity at $u = -\frac{1}{3}$ on the triangular lattice with the exact relation (2.12). Since the exponents $\alpha'_{\ell,\mathrm{FM}}$ and β_ℓ in (6.1) have twice the value of the respective exponents for the corresponding singularity at $u = -\frac{1}{3}$ on the triangular lattice, and the same is true of the inferred exact values $\gamma'_{\ell,\mathrm{FM}} = \frac{5}{2}$ from the present work and $\gamma'_e = \frac{5}{4}$ from [6], the right-hand side is also twice the value of 2 which holds for the triangular lattice.

One may also consider the analogous equation for the approach to $z = -1$ from within the complex-temperature extension of the AFM phase. We have extracted the exact value $\alpha'_{\ell,\mathrm{AFM}} = 2$ in (3.14) and, as discussed above, given the loose-packed nature of the

honeycomb lattice and the resultant relation (4.8), it follows that the staggered magnetization diverges with the exponent $\beta_{\ell,\text{st}} = \beta_\ell = -\frac{1}{4}$ as one approaches the point $z = -1$ from within the complex-temperature AFM phase. Combining these exact results with the inferred exact value $\gamma'_{\ell,a} = \frac{5}{2}$ from our analysis of the low-temperature series for the staggered susceptibility, we find

$$\alpha'_{\ell,\text{AFM}} + 2\beta_{\ell,\text{st}} + \gamma'_{\ell,a} = 4 \tag{6.2}$$

in complete analogy with (6.1), as expected for a loose-packed lattice.

7. Behaviour of $\bar{\chi}$ in the symmetric phase

The theorem proved in [7] and discussed further in [9] implies that, for the Ising model on the square lattice, $\bar{\chi}$ has at most finite non-analyticities as one approaches the boundary of the complex-temperature extension of the PM phase, aside from the physical critical point at $v = v_c$. We would expect a similar theorem to hold for the triangular and honeycomb lattices, although to show this with complete rigour, it would be desirable to perform an analysis of the asymptotic behaviour of the general connected two-spin correlation function $\langle \sigma_{0,0} \sigma_{m,n} \rangle$ as $r = (m^2 + n^2)^{1/2} \to \infty$ for this lattice. This has not, to our knowledge, been done (although some specific correlation functions on the triangular lattice have been computed in [37]). Assuming that such a theorem does hold, it would follow, in particular, that $\bar{\chi}_t(v)$ would have finite non-analyticities as one approaches the points $v = \pm i$ from within the PM phase. We have analysed the high-temperature series expansion for $\bar{\chi}_t(v)$ to investigate the singularities at $v = \pm i$. This series is of the form $\bar{\chi}_t = 1 + \sum_{n=1}^{\infty} a_{n,t} v^n$. It has a finite radius of convergence and, by analytic continuation from the physical high-temperature interval $0 \leqslant v < v_c$, applies throughout the complex extension of the PM phase. The high-temperature series expansion of $\bar{\chi}_t$ is known to $O(v^{16})$ [38, 26]. Since we anticipated a finite singularity, we analysed this series using differential approximants, which are capable of representing this type of singularity in the presence of an analytic background term. Mainly because of the shortness of the series, our study did not yield a definite value for the exponent γ_s at the points $v = \pm i$ corresponding to the point $u = -1$ as approached from within the complex PM phase. This might be possible with a substantially longer high-temperature series.

For the honeycomb lattice we performed a similar analysis on the high-temperature series for $\bar{\chi}_{\text{hc}}(v)$ and $\bar{\chi}_{\text{hc}}^{(a)}(v) = \bar{\chi}_{\text{hc}}(-v)$. The high-temperature series for $\bar{\chi}_{\text{hc}}(v)$ is related to that for $\bar{\chi}_t(v)$ by (2.14) and has been calculated to $O(v^{32})$ [38, 26]. However, there are two semi-infinite line segments which protrude into the complex-temperature PM phase, with endpoints at $v = \pm v_e = \pm i/\sqrt{3}$ (the phase diagram for the hc lattice is given by figure 1(*b*) with the replacements $z \to v$, FM $\leftrightarrow$ PM, and O $\to$ AFM). We found that the series are not sensitive to the singularities at $v = \pm i$, presumably because of the effect of the intervening singular line segments and their endpoints at $v = \pm i\sqrt{3}$. We have also tried to study the singularities in $\bar{\chi}$ at these endpoints. Again, our study did not yield an accurate value for the exponent γ_e, presumably due to the insufficient length of the series. However, the (scattered) values of γ_e were consistent with the expectation that $\gamma_e < 0$.

8. Conclusions

In this paper we have investigated complex-temperature singularities in the Ising model on the triangular and honeycomb lattices. As part of this, we have discussed the complex-temperature phases and their boundaries. From exact results, we have determined these

singularities completely for the specific heat and the uniform and staggered magnetization. For the singularity at $u = -\frac{1}{3}$, we have extended the previous study by Guttmann [6] with the use of differential approximants and have found excellent agreement with his results. We also discussed the implications of the divergence in the spontaneous magnetization at this point. For the honeycomb lattice, from an analysis of low-temperature series expansions, we have found evidence that χ and $\chi^{(a)}$ both have divergent singularities at $z = -1 \equiv z_\ell$, and our numerical values for the exponents are consistent with the hypothesis that the exact values are $\gamma'_\ell = \gamma'_{\ell,a} = \frac{5}{2}$. The critical amplitudes at this singularity were calculated. We have found that the relation $\alpha' + 2\beta + \gamma' = 2$ is violated at $z = -1$; the right-hand side is numerically consistent with being equal to 4. The connection between the exponents at $z = -1$ on the honeycomb and the exponents at the corresponding point $u = -\frac{1}{3}$ on the triangular lattice was discussed. Finally, we have commented on non-analyticities of $\bar{\chi}$ which could occur as one approaches the boundary of the symmetric phase from within that phase.

Acknowledgments

References

[1] Fisher M E 1965 *Lectures in Theoretical Physics* vol 7C (Boulder, CO: University of Colorado Press) p 1
[2] Katsura S 1967 *Prog. Theor. Phys.* **38** 1415
     Abe Y and Katsura S 1970 *Prog. Theor. Phys.* **43** 1402
[3] Ono S, Karaki Y, Suzuki M and Kawabata C 1968 *J. Phys. Soc. Japan* **25** 54
[4] Thompson C J, Guttmann A J and Ninham B W 1969 *J. Phys. C: Solid State Phys.* **2** 1889
     Guttmann A J 1969 *J. Phys. C: Solid State Phys.* **2** 1900
[5] Domb C and Guttmann A J 1970 *J. Phys. C: Solid State Phys.* **3** 1652
[6] Guttmann A J 1975 *J. Phys. A: Math. Gen.* **8** 1236
[7] Marchesini G and Shrock R 1989 *Nucl. Phys.* B **318** 541
[8] Enting I G, Guttmann A J and Jensen I 1994 *J. Phys. A: Math. Gen.* **27** 6963
[9] Matveev V and Shrock R 1995 *J. Phys. A: Math. Gen.* **28** 1557
[10] van Saarloos W and Kurtze D 1984 *J. Phys. A: Math. Gen.* **17** 1301
     Stephenson J and Couzens R 1984 *Physica* **129A** 201
     Wood D 1985 *J. Phys. A: Math. Gen.* **18** L481
     Stephenson J and van Aalst J 1986 *Physica* **136A** 160
[11] Maillard J M and Rammal R 1983 *J. Phys. A: Math. Gen.* **16** 353
[12] Martin P P 1991 *Potts Models and Related Problems in Statistical Mechanics* (Singapore: World Scientific)
[13] Hansel D and Maillard J-M 1988 *J. Phys. A: Math. Gen.* **21** 213
     Guttmann A J work in progress
[14] Onsager L 1944 *Phys. Rev.* **65** 117
[15] Houtappel R M F 1950 *Physica* **16** 425
     Husimi K and Syozi I 1950 *Prog. Theor. Phys.* **5** 177
     Syozi I 1950 *Prog. Theor. Phys.* **5** 341
     Newell G F 1950 *Phys. Rev.* **79** 876
     Temperley H N V 1950 *Proc. R. Soc.* A **202** 202
     Wannier G H 1950 *Phys. Rev.* **79** 357
     See also Potts R B 1955 *Proc. Phys. Soc.* A **68** 145
[16] Yang C N 1952 *Phys. Rev.* **85** 808
[17] Potts R B 1952 *Phys. Rev.* **88** 352

[18] Naya S 1954 *Prog. Theor. Phys.* **11** 53

[19] Domb C 1960 *Adv. Phys.* **9** 149

[20] Lefschetz S 1953 *Algebraic Geometry* (Princeton, NJ: Princeton University Press)
Hartshorne R 1977 *Algebraic Geometry* (New York: Springer)

[21] Fisher M E 1959 *Phys. Rev.* **113** 969

[22] Gradshteyn I S and Ryzhik I M 1980 *Table of Integrals, Series, and Products* (New York: Academic)
equation (8.128.1)

[23] Sykes M F, Essam J W and Gaunt D S 1965 *J. Math. Phys.* **6** 283 and references therein

[24] Sykes M F, Gaunt D S, Martin J L, Mattingly S R and Essam J W 1973 *J. Math. Phys.* **14** 1071

[25] Sykes M F, Watts M G and Gaunt D S 1975 *J. Phys. A: Math. Gen.* **8** 1448

[26] Gaunt D S 1994 Private communication

[27] Guttmann A J 1994 Private communication

[28] Barouch E, McCoy B and Wu T T 1973 *Phys. Rev. Lett.* **31** 1409
Wu T T, McCoy B, Tracy C A and Barouch E 1976 *Phys. Rev.* B **13** 316

[29] Barma M and Fisher M E 1985 *Phys. Rev.* B **31** 5954

[30] Guttmann A J 1989 *Phase Transitions and Critical Phenomena* vol 13 ed C Domb and J Lebowitz (New York: Academic)

[31] Essam J W and Fisher M E 1963 *J. Chem. Phys.* **38** 1802

[32] Guttmann A J 1973 *Phys. Rev.* B **9** 4991

[33] Betts D D, Guttmann A J and Joyce G S 1971 *J. Phys. C: Solid State Phys.* **4** 1994

[34] Thompson C J and Guttmann A J 1975 *Phys. Lett.* **53A** 315
Guttmann A J 1977 *J. Phys. A: Math. Gen.* **10** 1911
Gaunt D S and Guttmann A J 1978 *J. Phys. A: Math. Gen.* **11** 1381

[35] Cheng H and Wu T T 1967 *Phys. Rev.* **164** 719

[36] Shrock R 1995 *Nucl. Phys. B (Proc. Suppl.)* **42** 776

[37] Stephenson J 1964 *J. Math. Phys.* **5** 1009; 1970 *J. Math. Phys.* **11** 413

[38] Sykes M F, Gaunt D S, Roberts P D and Wyles J A 1972 *J. Phys. A: Math. Gen.* **5** 624